^{11}C-PK11195 PET for the In Vivo Evaluation of Neuroinflammation in the Rat Brain After Cortical Spreading Depression

Yilong Cui[1], Tadayuki Takashima[2], Misato Takashima-Hirano[3], Yasuhiro Wada[2], Miho Shukuri[4], Yasuhisa Tamura[1], Hisashi Doi[3], Hirotaka Onoe[4], Yosky Kataoka[1], and Yasuyoshi Watanabe[2]

[1]Cellular Function Imaging Laboratory, RIKEN Center for Molecular Imaging Science, Kobe, Hyogo, Japan; [2]Molecular Probe Dynamics Laboratory, RIKEN Center for Molecular Imaging Science, Kobe, Hyogo, Japan; [3]Molecular Imaging Labeling Chemistry Laboratory, RIKEN Center for Molecular Imaging Science, Kobe, Hyogo, Japan; and [4]Functional Probe Research Laboratories, RIKEN Center for Molecular Imaging Science, Kobe, Hyogo, Japan

Neurogenic inflammation triggered by extravasation of plasma protein has been hypothesized as a key factor in the generation of the pain sensation associated with migraine. The principal immune cell that responds to this inflammation is the parenchymal microglia of the central nervous system. **Methods:** Using a PET technique with ^{11}C-(*R*)-[1-(2-chlorophenyl)-*N*-methyl-*N*-(1-methylpropyl)-3-isoquinolinecarboxamide] (^{11}C-PK11195), a PET ligand for peripheral type–benzodiazepine receptor, we evaluated the microglial activation in the rat brain after generation of unilateral cortical spreading depression, a stimulation used to bring up an experimental animal model of migraine. **Results:** We found a significant increase in the brain uptake of ^{11}C-PK11195, which was completely displaceable by the excess amounts of unlabeled ligands, in the ipsilateral hemisphere of the spreading depression–generated rats. Moreover, the binding potential of ^{11}C-PK11195 in the spreading depression–generated rats was significantly higher than that in the sham-operated control rats. **Conclusion:** These results suggest that as an inflammatory reaction, microglial cells are activated in response to the nociceptive stimuli induced by cortical spreading depression in the rat brain. Therefore, the ^{11}C-PK11195 PET technique could have a potential for diagnostic and therapeutic monitoring of neurologic disorders related to neuroinflammation such as migraine.

Key Words: binding potential; microglia; peripheral benzodiazepine receptor; migraine

J Nucl Med 2009; 50:1904–1911
DOI: 10.2967/jnumed.109.066498

Neuroinflammation is a process whereby glial cells are activated in response to infection, disease, or injuries involved in the central nervous system. Such inflammatory reactions are implicated in several neurologic disorders such as migraine, Alzheimer disease, stroke, Parkinson disease, brain trauma, spinal cord injury, and multiple sclerosis (*1,2*). Neurogenic inflammation has been implicated as a key factor in the generation of the pain sensation associated with migraine headaches (*3–5*). It is hypothesized that the proinflammatory peptides, such as substance P and calcitonin gene–related peptide, released from trigeminocervical nerve terminals in response to meningeal nociceptive stimuli, induce vasodilation and plasma protein extravasation. Such neurogenic inflammatory reactions were thought to trigger headache via a stimulation of trigeminal afferents (*4,5*). Consistent with this theory, vasogenic leakage (*6,7*) and an increase in calcitonin gene–related peptide in the jugular vein (*8*) have been reported in migraine patients during migraine attack. However, recent clinical trials have shown that several drugs that selectively inhibit plasma protein extravasation in rodents have failed to reduce pain severity in patients with migraine (*9*). These observations indicate that a noninvasive evaluation method for neuroinflammation is necessary to investigate whether and how the neuroinflammation is involved in migraine etiology and verify the extrapolated data from an animal study to the human condition.

As the principal immune cells in the central nervous system, the microglial cells are activated in response to such neurogenic inflammation. The process of microglial activation is thought to be related to an increase in the number of microglial cells and the expression of numerous proteins such as peripheral benzodiazepine receptor (PBR) (*10*). The PBR, which is a mitochondrial outer membrane protein and is expressed at low levels in the normal brain on resting microglial cells and astrocytes, is known to be upregulated in the activated microglial cells (*11–13*). ^{11}C-labeled PK11195, a ligand that specifically binds to PBR, has been used extensively for imaging of activated microglial cells by PET in several neurologic disorders, such as stroke (*14*), multiple sclerosis (*15*), Alzheimer disease (*16*), Parkinson disease (*17*), and Huntington disease (*18*). However, no literature has described the

Received May 22, 2009; revision accepted Aug. 17, 2009.
Correspondence or reprints contact: Yilong Cui, Cellular Function Imaging Laboratory, RIKEN Center for Molecular Imaging Science, 6-7-3 Minatojima Minamimachi, Chuo-ku, Kobe, Hyogo 650-007, Japan.
E-mail: cuiyl@riken.jp

microglial activation in the brain of migraine patients using PET with ^{11}C-PK11195.

Cortical spreading depression, described first by Leao (*19*) in 1944, is implicated in the pathogenesis of migraine. Cortical spreading depression is characterized by the spreading of neuronal or glial membrane depolarization accompanied by temporal elevation of the cerebral blood flow (CBF) throughout the cerebral cortical hemisphere at a rate of 2–5 mm/min (*20,21*). The rate of spread correlates with the observed spread of the aura of classic migraine (*22*), which is characterized by either a paracentral scotoma or a small scintillating area of bright light. A spreading oligemia has been observed at a similar velocity during migraine attacks in experimental cortical spreading depression models (*23,24*). Hadjikhani et al. (*25*) also reported that a neurovascular event closely resembling cortical spreading depression has been shown with functional MRI during the migraine visual aura. On the basis of these observations and other experimental data, the cortical spreading depression has been hypothesized as an endogenous event involved in migraine etiology (*26,27*). In this study, we used ^{11}C-PK11195 PET to investigate the neurogenic inflammation in the cerebral cortex induced by unilateral cortical spreading depression.

MATERIALS AND METHODS

All experimental protocols were approved by the Ethics Committee on Animal Care and Use of the Institute of Physical and Chemical Research and were performed in accordance with the *Guide for the Care and Use of Laboratory Animals* (*28*).

Chemicals

(*R*)-[1-(2-chlorophenyl)-*N*-methyl-*N*-(1-methyl-propyl)-3-isoquinoline-carboxamide] ((*R*)-*N*-desmethyl-PK11195) was obtained from Advanced Biochemical Compounds (ABX). ^{11}C-labeled PK11195 was synthesized according to the procedures described by Shah et al. (*29*), with slight modifications. Briefly, 1 mg of (*R*)-*N*-desmethyl-PK11195 was dissolved in 200 μL of anhydrous dimethyl sulfoxide, containing 1 mg of KOH. After trapping of the ^{11}C-CH_3I, the vial was heated at 90°C for 4 min. Purification was performed by high-performance liquid chromatography on a COSMOSIL C_{18}-AR-II column (10 × 250 mm, 5-μm particle size) (Nakalai) using acetonitrile:water (70:30) as the mobile phase. The purified fraction was evaporated to dryness and reconstituted with 4 mL of a saline solution including 0.3 mL of propylene glycol and 0.05 mL of polysorbate 80. The specific activity ranged from 30 to 70 GBq/μmol. Radiochemical purity was higher than 99%.

Animal Preparation for Generation of Spreading Depression

Male Sprague–Dawley rats (SLC), weighing approximately 300 g, were used. To prepare the spreading depression rat model, the head of each rat was fixed in a stereotactic apparatus (type 1430, David Kopf) under 1.5% isoflurane anesthesia. A thermocouple probe was connected with a thermocontroller and inserted into the rectum to maintain the body temperature at 37°C. A small burr hole was drilled in the skull at the frontal cortex (2.0–3.0 mm anterior and 2.0–3.0 mm lateral to the bregma). A glass micropipette (internal diameter of the tip, 50 μm) was inserted 1 mm below the cortical surface through the burr hole for subsequent microinjection. Two hours after the insertion, a microinjection of 1 M KCl was performed (at a rate of 0.2 μL/min for 1 min) every 10 min for a period of 2 h (12 injections; 2.4 μL of total volume). Sham controls (n = 4 animals) were injected with 1 M NaCl at an analogous rate, duration, and frequency.

A laser Doppler flowmetry (LDF) (type FLO-N1; ω-wave) probe was stereotactically placed in the parietal cortex over the skull for recording changes in CBF. The absolute value from LDF does not mean actual perfusion units; therefore, relative change in CBF is displayed (the data are normalized to prelevel).

PET Studies

Rats (n = 39) were anesthetized and maintained with a mixture of 1.5% isoflurane and nitrous oxide and oxygen (7:3) and positioned in the gantry of a PET scanner (microPET Focus 220; Siemens Co., Ltd.). After a bolus injection of ^{11}C-PK11195 (~100 MBq per animal) via a tail vein, a 60-min emission scan was performed with 400–650 keV as the energy window and 6 ns as the coincidence time window. Unlabeled ligands (n = 4, 1 mg/kg) were injected intravenously 20 min after the injection of radiotracers for the displacement experiment. Emission data were acquired in the list mode. The acquired data were sorted into single sinogram (for static image) and dynamic sinograms (6 × 10 s, 6 × 30 s, 11 × 60 s, and 15 × 180 s, for a total of 38 frames). The data were reconstructed by standard 2-dimensional filtered backprojection (FBP) with ramp filter and cutoff frequency at 0.5 cycles per pixel or by a statistical maximum a posteriori probability (MAP) algorithm (12 iterations with point spread function effect). Compared with FBP, MAP-reconstructed images have been shown to result in improved spatial resolution and noise properties on small-animal PET images, an advantage for image coregistration. Meanwhile, FBP-reconstructed images were used for quantification. The radioactivity concentrations were normalized with cylinder phantom data and were expressed as standardized uptake values.

Image Analysis

A 3-dimensional T2-weighted MRI template, which was aligned in space with the rat brain atlas of Paxinos (*30*), was used for defining regions of interest (ROIs). PET images were manually coregistered with the MRI template using an image-processing small-animal PET software package (ASIPro 6.05; Siemens Co., Ltd.). ROIs were defined for each rat on the region of microinjection (core, as delineated by the hypersignal seen in the MAP-reconstructed image), ipsilateral surrounding areas (ipsilateral), and corresponding contralateral areas (contralateral, as shown in Fig. 1). Each region was primarily drawn on coronal slices and then confirmed on sagittal and horizontal slices. All related ROIs were stacked into the volume of interest (VOI), and the mean value in each VOI was used to generate regional time–activity curves.

Radioactivity and Metabolite Analysis in Plasma

Arterial blood was collected from the femoral artery at 10, 20, 30, 40, 50, and 60 s and 2, 5, 10, 25, and 40 min after administration. The radioactivity of blood and plasma was measured by a well-type γ-counter (Wallac1470; PerkinElmer) and corrected for decay. For the metabolite analysis, plasma

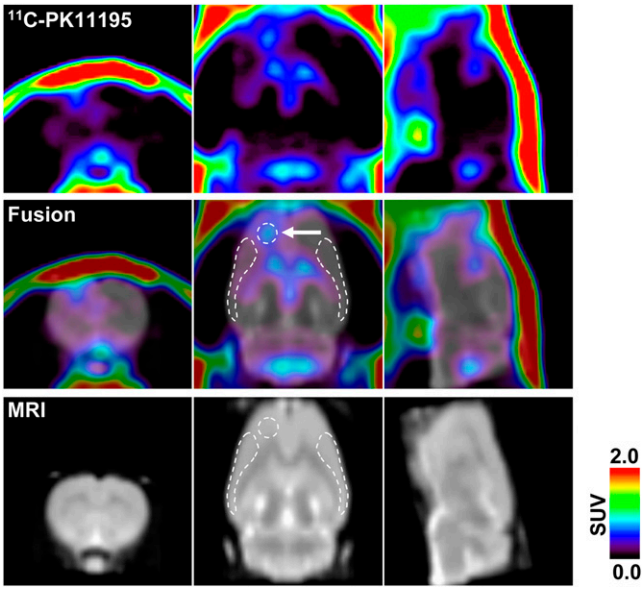

FIGURE 1. Representative ^{11}C-PK11195 PET image coregistered with MRI template 8 d after generation of unilateral (left hemisphere) cortical spreading depression. PET image was reconstructed with MAP algorithm and summated from 5 to 60 min after radioligand injection. Arrow in middle panel indicates KCl-microinjected area (core). White broken lines in middle and bottom panels indicate ROIs (core, ipsilateral, and contralateral, respectively) defined in this study.

samples (1, 2, 5, 10, 25, and 40 min after administration) were extracted by acetonitrile, and the extracts were applied to an RP-18 thin-layer chromatography (TLC) plate (Merck). The plate was developed with acetonitrile:water (70:30) as the mobile phase. After migration, the TLC plates were dried and exposed on imaging plates (BAS TR2040; Fuji Photo Film) for 40 min. The signal of radioactivity on the imaging plates was measured with a digital PSL autoradiography analyzer (FLA-7000; Fuji Photo Film), and the data were estimated using imaging-analysis software (MultiGauge; Fuji Photo Film).

Kinetic Analysis

Kinetic modeling was performed using the PMOD software package (version 2.85; PMOD Technologies). A metabolite-corrected plasma input function was obtained by fitting to an exponential function, as follows. The ^{11}C-PK11195 parent fraction in the plasma samples for each sampling point was multiplied by this exponential function to obtain the metabolite-corrected plasma input function. The metabolite-corrected plasma time–activity curves were fitted to 2 exponential functions to obtain the plasma pharmacokinetic parameter. The standard input function was obtained by averaging individual input functions from 3 satellite rats, and k_2' of the reference region (contralateral hemisphere), which represents the clearance from the reference region into the vascular compartment, was obtained using a 1-tissue-compartment model for each animal imaged. The averaged k_2' estimated in this study was 0.14/min. Binding potential (BP) was calculated for ipsilateral ROI kinetics using Logan noninvasive graphical analysis (*31*), which was applied to the target regions by the following equation:

$$\frac{\int_0^T C(t)dt}{C(T)} = DVR\left[\frac{\int_0^T C'(t)dt + C'(T)/k_2'}{C(T)}\right] + int',$$

where $C(T)$ is the radioactivity concentration in the tissue of interest, and $C'(T)$ is the radioactivity concentration in the reference tissue (contralateral ROI). DVR is the distribution volume ratio calculated by the regression slope, int′ is an intercept that becomes constant after an equilibration, and k_2' is the average tissue-to-plasma clearance, which has to be determined before this analysis. In this study, k_2' was determined directly using the standard input function as shown above. Finally, BP is evaluated as BP = DVR − 1.

Immunohistochemistry

The level of microglial activation was investigated by immunohistochemistry in the spreading depression–generated (n = 4) and sham control (n = 4) rats at 8 d after the operation. After the PET scan, the rats were anesthetized and perfused with 4% formaldehyde buffered with 0.1 M phosphate-buffered saline (pH 7.4). The brain was removed and further fixed in the same fixative at 4°C for 24 h. We prepared coronal brain sections (30-μm thickness) using a cryostat. To immunostain the microglial cells, mouse monoclonal antibody against rat OX-42 (1:100; Abcam) was used. The bound antibodies were visualized by the avidin–biotin complex method (Vectastain ABC kit; Vector) with 3, 3′-diaminobenzidine.

Data Analysis

All results were expressed as mean ± SD. The statistical differences in BP values between spreading depression–generated and sham-operated groups were assessed by 2-tailed unpaired t test. The statistical significance was set at P less than 0.05.

RESULTS

Spreading Depression in Rat Cerebral Cortex

Occurrence of cortical spreading depression in all rats used for the PET study was evaluated by transient CBF hyperperfusion recorded continuously from the ipsilateral hemisphere (7 mm posterior to the injection site). Transient CBF hyperperfusion always occurred after microinjection of 1 M KCl (at a rate of 0.2 μL/min for 1 min) in the ipsilateral hemisphere (Fig. 2), as is characteristic of spreading depression (*21*). Such transient CBF hyperperfusions are well known to be synchronously accompanied by the transient negative shifts of direct current (DC) potential, as described in our previous report (*21*) and in other literature (*32*). The mean number of transient hyperperfusions in the KCl-treated rats (n = 35) was 12.8 ± 3.3 over 2 h. However, microinjection of 1 M NaCl (n = 4) in an analogous fashion did not induce similar changes in CBF, indicating that cortical spreading depression was not induced in those rats.

PET Studies

To investigate the neurogenic inflammation after cortical spreading depression, we examined microglial activation using ^{11}C-PK11195 PET at 1, 3, 8, and 15 d after induction

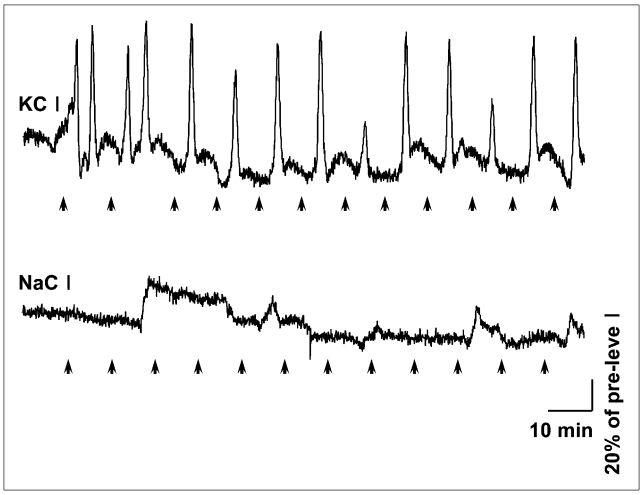

FIGURE 2. Cortical spreading depression–associated CBF changes in experimental and sham-operated rat. Dynamic changes in CBF were continuously recorded from parietal cortex over skull using LDF. Upper panel shows a representative CBF change recorded from parietal cortex in KCl-microinjected rat. Lower panel shows result from a rat who received NaCl microinjection using analogous paradigm, as sham operation. Arrows at bottom of each panel indicate time of microinjection. Note that spreading depression–associated CBF hyperperfusions were not observed in sham-operated rat.

of unilateral cortical spreading depression in the rats. The radioactivity of ^{11}C-PK11195 was barely observed within the brain under normal condition in the control rats, except for the cerebral ventricles, including the lateral ventricle, third ventricle, and fourth ventricle (data not shown). In the cortical spreading depression–generated rats, ^{11}C-PK11195 radioactivity was high in the ipsilateral hemisphere, as compared with that in the contralateral hemisphere. The ^{11}C-PK11195 radioactivity was detectable in the injection site 1 d after the KCl treatment, and that increased and spread extensively in the ipsilateral surrounding areas at 3, 8, and 15 d after the KCl treatment (Figs. 1 and 3). Figure 1 shows a representative ^{11}C-PK11195 PET image coregistered with the corresponding MR image at 8 d after the KCl treatment. The highest radioactivity was seen in the KCl-microinjected site (core), and moderate radioactivity was observed in the ipsilateral surrounding areas but not in the corresponding contralateral areas (Fig. 1). In the sham control rats, however, a slight increase in ^{11}C-PK11195 radioactivity was seen primarily in the NaCl-microinjected site at 8 d after the sham operation.

The temporal changes of ^{11}C-PK11195 uptake in the core, ipsilateral, and contralateral ROIs were similar (Fig. 3). The radioactivity of ^{11}C-PK11195 in the contralateral ROI reached a peak within the first minute after radiotracer injection and decreased rapidly thereafter. In the cortical spreading depression–generated rats, the decrement in the ipsilateral areas (core and ipsilateral ROIs) was slower than that in the contralateral areas (contralateral ROI). The obvious contrast of radioactivity between ipsi- and contralateral hemispheres appeared first 3 d after the operation and remained until the end of the study (Fig. 3). No obvious contrast between the 2 hemispheres was observed in the sham-operated control rats at 8 d after the NaCl treatment.

In vivo displacement was performed by injecting unlabeled PK11195 (n = 4, 1 mg/kg) at 20 min after the injection of ^{11}C-PK11195 (Fig. 4). Immediately after injection of unlabeled PK11195, the brain uptake of ^{11}C-PK11195 was transiently increased in both ipsi- and contralateral hemispheres because of a release of ^{11}C-PK11195 from peripheral organs into the blood circulation, as previously reported (*33,34*). The contrast of radioactivity between the 2 hemispheres completely disappeared after the unlabeled PK11195 injection, indicating ^{11}C-PK11195 was rapidly displaced by unlabeled PK11195 in the ipsilateral hemisphere.

Using Logan noninvasive graphical analysis, we estimated the BP value for ^{11}C-PK11195 in the core and ipsilateral ROIs. The BP values in the core and ipsilateral ROIs were increased with the time after the KCl treatment (Fig. 5). In the cortical spreading depression–generated rats, the mean value of BP in the core ROI reached 0.45 ± 0.10 (n = 5) at 3 d after the KCl treatment and maintained approximately the same level until 15 d (0.51 ± 0.36, n = 5). The mean values in the ipsilateral ROI were approximately half of those in the core ROI at each time of the examination, indicating that microglial activation was outstanding in the microinjected site. In contrast with the cortical spreading depression–generated rats, the BP values were lower in the sham-operated control (NaCl treatment) rats. Significant differences between spreading depression–generated and sham control rats were noted in both ROIs at 8 d after the operation (core, 0.48 ± 0.18 vs. 0.21 ± 0.05, and ipsilateral, 0.26 ± 0.07 vs. 0.14 ± 0.08, in the spreading depression–generated [n = 11] and sham control [n = 4] rats, respectively; $P < 0.05$, unpaired t test) (Fig. 6).

Immunohistochemical Studies

The activation of microglial cells was confirmed by immunohistochemical studies after the induction of spreading depression. As shown in Figure 7, a large number of immunosignals of OX-42 were observed in the ipsilateral hemisphere, compared with the corresponding area of the contralateral hemisphere, in the rats 8 d after unilateral spreading depression generation. Magnified photomicrographs taken from the corresponding parietal cortex showed that hypertrophied (enlarged, darkened soma with shorter, thicker processes) or ameboid (densely stained, enlarged soma with a few short processes) OX-42–positive microglial cells were often seen in the ipsilateral hemisphere (Fig. 7C). However, such a difference between the 2

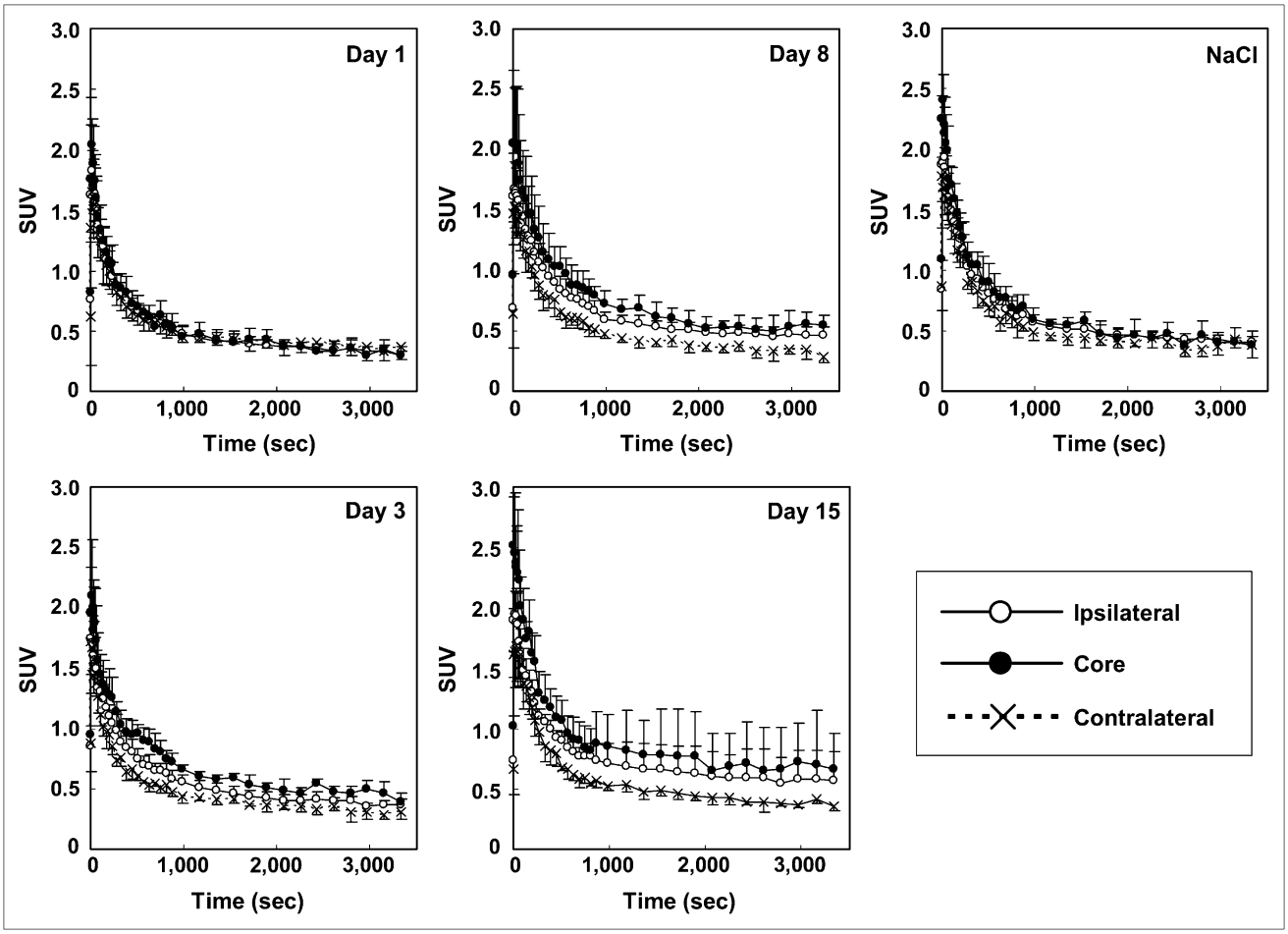

FIGURE 3. Time–activity curves for ^{11}C-PK11195 in brain regions of experimental (at 1, 3, 8, and 15 d after microinjection of KCl) and sham-operated (8 d after microinjection of NaCl) rats. Data were expressed as mean ± SD.

hemispheres was not observed in the rats treated with NaCl as a sham operation.

DISCUSSION

Neurogenic inflammation is thought to be a key factor in the generation of pain sensation in migraine headaches. In the present study, we evaluated neurogenic inflammation using an animal model of migraine and noninvasive PET. Our results show that in the unilateral spreading depression model rats, the uptake of ^{11}C-PK11195, a PET tracer for PBR, which is used extensively to image activated microglial cells in the central nervous system, was increased in the ipsilateral hemisphere and completely displaced by excess unlabeled ligands. In addition, quantitative analysis in spreading depression model rats, compared with that in the sham-operated control rats, showed that the BP values in the core and ipsilateral ROIs were significantly high. Finally, predominant microglial activation in the ipsilateral cerebral hemisphere of the spreading depression model rats was also confirmed by immunohistochemical study. These observations suggest that an inflammatory process may be involved in the pathologic state of migraine and that ^{11}C-PK11195 PET is a useful tool for evaluating the neurogenic inflammation in vivo.

On the basis of the expression pattern of the PBR in the pathophysiologic state, ^{11}C-labeled PK11195 has been developed as a specific PET ligand for the PBR to image activated microglial cells in the brain (*15,17,35,36*). The PBR is known to be highly expressed in activated microglial cells under neuropathologic conditions but barely expressed in healthy brain tissue (*12,13*). The upregulated level of PBR was known to be well correlated with the state of microglial activation (*15,37,38*). In the present study, we used unilateral cortical spreading depression as an animal model of migraine and demonstrated that the brain uptake of ^{11}C-PK11195 was specifically increased in the ipsilateral hemisphere. It is well known that cortical spreading depression–induced pathophysiologic changes, such as transient CBF hyperperfusion, negative DC potential shifts, and related biochemical events, are restricted to the ipsilateral hemisphere (*19,21,39*). Consistent with these characteristics of spreading depression, we demonstrated that micro-

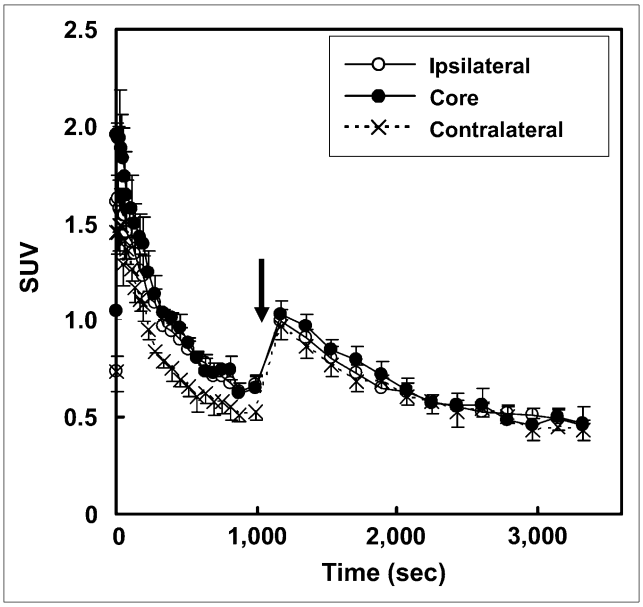

FIGURE 4. Time–activity curves for ^{11}C-PK11195 displaced by excess unlabeled PK11195 in brain regions 8 d after generation of unilateral cortical spreading depression. Unlabeled PK11195 (n = 4, 1 mg/kg) was administered 20 min after injection of radioligand. Arrow indicates time of injection of unlabeled ligand. Data were expressed as mean ± SD.

glial reactivity, indicated by immunosignal of OX-42, was observed predominantly in the ipsilateral hemisphere after cortical spreading depression. Indeed, Caggiano et al. (*40*) have also reported that reactive microglial cells appeared predominantly in the ipsilateral hemisphere after KCl-induced unilateral neocortical spreading depression by the immunohistochemical approach. Moreover, our displacement experiment demonstrated that such a superior brain

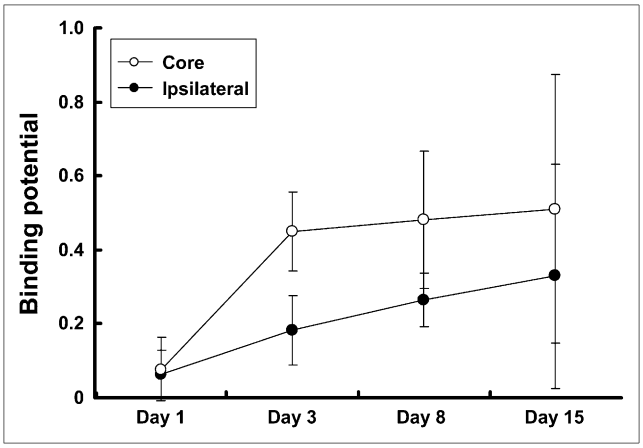

FIGURE 5. BP for ^{11}C-PK11195 in core and ipsilateral ROIs at 1, 3, 8, and 15 d after induction of unilateral cortical spreading depression by KCl microinjection. BP values were estimated in core and ipsilateral ROIs using Logan noninvasive graphical analysis. Corresponding contralateral ROI was used as reference. Data were expressed as mean ± SD.

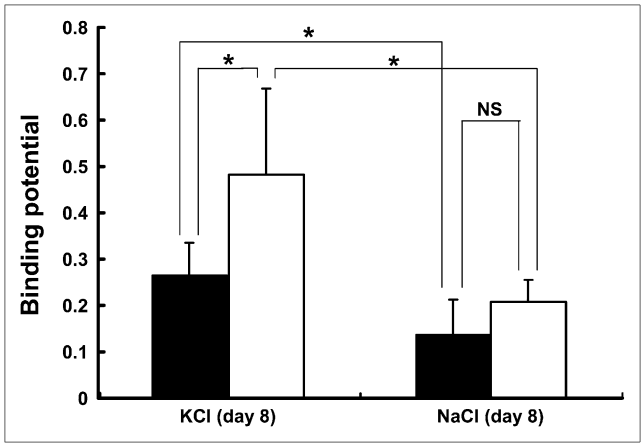

FIGURE 6. Comparison of BP for ^{11}C-PK11195 in ROIs (core and ipsilateral) between experimental and sham-operated rats. BP values were estimated from experimental (KCl microinjection, n = 11) and sham-operated (NaCl microinjection, n = 4) rats 8 d after operation. Open and closed bars indicate core and ipsilateral ROIs, respectively. Data were expressed as mean ± SD. NS = not significant. *$P < 0.05$, unpaired t test.

uptake of ^{11}C-PK11195 in the ipsilateral hemisphere was completely displaced by excess unlabeled ligands. Though astrocytes have also been reported to express PBR in vitro (*41*), the origin of ^{11}C-PK11195 radioactivity in vivo is thought to be primarily from activated microglial cells in the brain (*15,35,36*). Therefore, the increased radioactivity of ^{11}C-PK11195 in the ipsilateral hemisphere may originate from the activated microglial cells in response to the neurogenic inflammation after the unilateral spreading depression.

In the present study, BP value for ^{11}C-PK11195 was estimated using the Logan noninvasive graphical analysis (*31*). The mean BP value for ^{11}C-PK11195 was approximately 0.5 in the core ROI after spreading depression generation. That value was slightly lower than that reported in the α-amino-3-hydroxy-5-methyl-4-isoxazole propionic acid–induced lesion area of the rat striatum (0.66 ± 0.15), in which the BP value was estimated by a simplified reference tissue model (*33*). Using the simplified reference tissue model, Cagnin et al. also have reported that mean BP value for ^{11}C-PK11195 in the cerebral cortex of healthy volunteers was 0.13 ± 0.04 and increased variably (≤0.79) in several cortical regions of patients with herpes simplex encephalitis (*36*). In the present study, the highest value of mean BP for ^{11}C-PK11195 was noted in the KCl-microinjected site (0.48 ± 0.18), and a moderate value was observed in the surrounding area of the injection site (0.26 ± 0.07) 8 d after the unilateral spreading depression generation. In contrast, the BP value in the ipsilateral hemisphere of sham-operated rats was 0.14 ± 0.08, which was almost equivalent to the value reported by Cagnin et al. for the cerebral cortex of healthy volunteers. (*36*). These

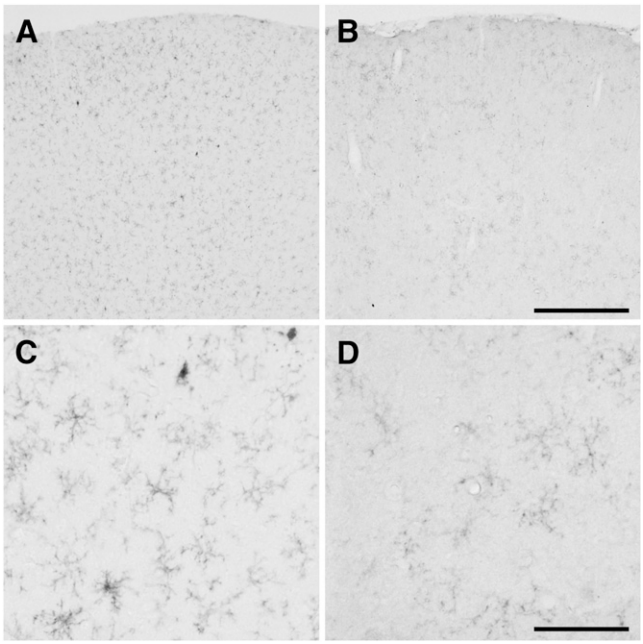

FIGURE 7. Photomicrographs of OX-42 immunoreactivity after cortical spreading depression. Images display OX-42 immunoreactivity 8 d after 2 h of recurrent spreading depression in left hemisphere (A and C), compared with contralateral hemisphere (B and D). (C and D) Magnified views of OX-42 immunoreactivity. Hypertrophied or ameboid OX-42–positive microglial cells were often seen in left hemisphere. Bars in B and D indicate 500 and 100 μm, respectively.

observations suggest that ^{11}C-PK11195 PET is potentially useful for the quantitative evaluation of temporal change in neurogenic inflammation in the rat model of migraine.

CONCLUSION

In the present study, we evaluated for the first time, to our knowledge, the neurogenic inflammation in the rat model of migraine using quantitative PET with ^{11}C-PK11195. The microglial activation quantified by ^{11}C-PK11195 PET was significantly increased in the cerebral hemisphere, which underwent unilateral cortical spreading depression. These results suggest that ^{11}C-PK11195 PET is useful for the evaluation of the neurogenic inflammatory process and may provide a new and powerful tool for both the diagnosis of migraine and the monitoring efficacy for migraine therapy.

ACKNOWLEDGMENT

This work was supported in part by a consignment expense from the Molecular Imaging Program on "Research Base for Exploring New Drugs" from the Ministry of Education, Culture, Sports, Science, and Technology (MEXT), Japanese government.

REFERENCES

1. Kreutzberg GW. Microglia: a sensor for pathological events in the CNS. *Trends Neurosci.* 1996;19:312–318.
2. Streit WJ, Mrak RE, Griffin WS. Microglia and neuroinflammation: a pathological perspective. *J Neuroinflammation.* 2004;1:14.
3. Dalessio DJ. A classification of headache. *Int Ophthalmol Clin.* 1970;10:647–665.
4. Markowitz S, Saito K, Moskowitz MA. Neurogenically mediated leakage of plasma protein occurs from blood vessels in dura mater but not brain. *J Neurosci.* 1987;7:4129–4136.
5. Moskowitz MA. The neurobiology of vascular head pain. *Ann Neurol.* 1984;16:157–168.
6. Arnold G, Reuter U, Kinze S, Wolf T, Einhaupl KM. Migraine with aura shows gadolinium enhancement which is reversed following prophylactic treatment. *Cephalalgia.* 1998;18:644–646.
7. Iizuka T, Sakai F, Suzuki K, Igarashi H, Suzuki N. Implication of augmented vasogenic leakage in the mechanism of persistent aura in sporadic hemiplegic migraine. *Cephalalgia.* 2006;26:332–335.
8. Goadsby PJ, Edvinsson L, Ekman R. Vasoactive peptide release in the extracerebral circulation of humans during migraine headache. *Ann Neurol.* 1990;28:183–187.
9. Peroutka SJ. Neurogenic inflammation and migraine: implications for the therapeutics. *Mol Interv.* 2005;5:304–311.
10. Moran LB, Duke DC, Turkheimer FE, Banati RB, Graeber MB. Towards a transcriptome definition of microglial cells. *Neurogenetics.* 2004;5:95–108.
11. Benavides J, Guilloux F, Rufat P, et al. In vivo labelling in several rat tissues of 'peripheral type' benzodiazepine binding sites. *Eur J Pharmacol.* 1984;99:1–7.
12. Cagnin A, Gerhard A, Banati RB. In vivo imaging of neuroinflammation. *Eur Neuropsychopharmacol.* 2002;12:581–586.
13. Casellas P, Galiegue S, Basile AS. Peripheral benzodiazepine receptors and mitochondrial function. *Neurochem Int.* 2002;40:475–486.
14. Price CJ, Wang D, Menon DK, et al. Intrinsic activated microglia map to the peri-infarct zone in the subacute phase of ischemic stroke. *Stroke.* 2006;37:1749–1753.
15. Banati RB, Newcombe J, Gunn RN, et al. The peripheral benzodiazepine binding site in the brain in multiple sclerosis: quantitative in vivo imaging of microglia as a measure of disease activity. *Brain.* 2000;123:2321–2337.
16. Cagnin A, Brooks DJ, Kennedy AM, et al. In-vivo measurement of activated microglia in dementia. *Lancet.* 2001;358:461–467.
17. Gerhard A, Pavese N, Hotton G, et al. In vivo imaging of microglial activation with [^{11}C](*R*)-PK11195 PET in idiopathic Parkinson's disease. *Neurobiol Dis.* 2006;21:404–412.
18. Pavese N, Gerhard A, Tai YF, et al. Microglial activation correlates with severity in Huntington disease: a clinical and PET study. *Neurology.* 2006;66:1638–1643.
19. Leao AAP. Spreading depression of activity in the cerebral cortex. *J Neurophysiol.* 1944;7:359–390.
20. Nedergaard M, Hansen AJ. Spreading depression is not associated with neuronal injury in the normal brain. *Brain Res.* 1988;449:395–398.
21. Cui Y, Kataoka Y, Li QH, et al. Targeted tissue oxidation in the cerebral cortex induces local prolonged depolarization and cortical spreading depression in the rat brain. *Biochem Biophys Res Commun.* 2003;300:631–636.
22. Milner PM. Note on a possible correspondence between the scotomas of migraine and spreading depression of Leao. *Electroencephalogr Clin Neurophysiol.* 1958;10:705.
23. Lauritzen M, Skyhoj Olsen T, Lassen NA, Paulson OB. Changes in regional cerebral blood flow during the course of classic migraine attacks. *Ann Neurol.* 1983;13:633–641.
24. Olesen J, Larsen B, Lauritzen M. Focal hyperemia followed by spreading oligemia and impaired activation of rCBF in classic migraine. *Ann Neurol.* 1981;9:344–352.
25. Hadjikhani N, Sanchez Del Rio M, Wu O, et al. Mechanisms of migraine aura revealed by functional MRI in human visual cortex. *Proc Natl Acad Sci USA.* 2001;98:4687–4692.
26. Eikermann-Haerter K, Moskowitz MA. Animal models of migraine headache and aura. *Curr Opin Neurol.* 2008;21:294–300.
27. Lauritzen M. Pathophysiology of the migraine aura: the spreading depression theory. *Brain.* 1994;117:199–210.
28. *Guide for the Care and Use of Laboratory Animals.* Washington, DC: Government Printing Office; 1985. NIH publication 85-23.
29. Shah F, Hume SP, Pike VW, Ashworth S, McDermott J. Synthesis of the enantiomers of [*N*-methyl-^{11}C]PK 11195 and comparison of their behaviours as radioligands for PK binding sites in rats. *Nucl Med Biol.* 1994;21:573–581.

30. Schweinhardt P, Fransson P, Olson L, Spenger C, Andersson JL. A template for spatial normalisation of MR images of the rat brain. *J Neurosci Methods.* 2003;129:105–113.
31. Logan J, Fowler JS, Volkow ND, Wang GJ, Ding YS, Alexoff DL. Distribution volume ratios without blood sampling from graphical analysis of PET data. *J Cereb Blood Flow Metab.* 1996;16:834–840.
32. Back T, Kohno K, Hossmann KA. Cortical negative DC deflections following middle cerebral artery occlusion and KCl-induced spreading depression: effect on blood flow, tissue oxygenation, and electroencephalogram. *J Cereb Blood Flow Metab.* 1994;14:12–19.
33. Boutin H, Chauveau F, Thominiaux C, et al. ^{11}C-DPA-713: a novel peripheral benzodiazepine receptor PET ligand for in vivo imaging of neuroinflammation. *J Nucl Med.* 2007;48:573–581.
34. Gulyas B, Halldin C, Vas A, et al. [^{11}C]vinpocetine: a prospective peripheral benzodiazepine receptor ligand for primate PET studies. *J Neurol Sci.* 2005; 229–230:219–223.
35. Banati RB, Goerres GW, Myers R, et al. [^{11}C](*R*)-PK11195 positron emission tomography imaging of activated microglia in vivo in Rasmussen's encephalitis. *Neurology.* 1999;53:2199–2203.
36. Cagnin A, Myers R, Gunn RN, et al. In vivo visualization of activated glia by [^{11}C] (*R*)-PK11195-PET following herpes encephalitis reveals projected neuronal damage beyond the primary focal lesion. *Brain.* 2001;124:2014–2027.
37. Stephenson DT, Schober DA, Smalstig EB, Mincy RE, Gehlert DR, Clemens JA. Peripheral benzodiazepine receptors are colocalized with activated microglia following transient global forebrain ischemia in the rat. *J Neurosci.* 1995; 15:5263–5274.
38. Vowinckel E, Reutens D, Becher B, et al. PK11195 binding to the peripheral benzodiazepine receptor as a marker of microglia activation in multiple sclerosis and experimental autoimmune encephalomyelitis. *J Neurosci Res.* 1997;50:345–353.
39. Cui Y, Kataoka Y, Inui T, et al. Up-regulated neuronal COX-2 expression after cortical spreading depression is involved in non-REM sleep induction in rats. *J Neurosci Res.* 2008;86:929–936.
40. Caggiano AO, Kraig RP. Eicosanoids and nitric oxide influence induction of reactive gliosis from spreading depression in microglia but not astrocytes. *J Comp Neurol.* 1996;369:93–108.
41. Itzhak Y, Baker L, Norenberg MD. Characterization of the peripheral-type benzodiazepine receptors in cultured astrocytes: evidence for multiplicity. *Glia.* 1993;9:211–218.